REPORT DOCUMENTATION PAGE

Form Approved OMB No. 0704-0188

1. REPORT DATE *(DD-MM-YYYY)*	2. REPORT TYPE	3. DATES COVERED *(From - To)*
	Technical Papers	

4. TITLE AND SUBTITLE

5a. CONTRACT NUMBER

5b. GRANT NUMBER

5c. PROGRAM ELEMENT NUMBER

6. AUTHOR(S)

5d. PROJECT NUMBER
3058

5e. TASK NUMBER
RF9A

5f. WORK UNIT NUMBER

7. PERFORMING ORGANIZATION NAME(S) AND ADDRESS(ES)

Air Force Research Laboratory (AFMC)
AFRL/PRS
5 Pollux Drive
Edwards AFB CA 93524-7048

8. PERFORMING ORGANIZATION REPORT

9. SPONSORING / MONITORING AGENCY NAME(S) AND ADDRESS(ES)

Air Force Research Laboratory (AFMC)
AFRL/PRS
5 Pollux Drive
Edwards AFB CA 93524-7048

10. SPONSOR/MONITOR'S ACRONYM(S)

11. SPONSOR/MONITOR'S NUMBER(S)

12. DISTRIBUTION / AVAILABILITY STATEMENT

Approved for public release; distribution unlimited.

13. SUPPLEMENTARY NOTES

14. ABSTRACT

15. SUBJECT TERMS

16. SECURITY CLASSIFICATION OF:			17. LIMITATION OF ABSTRACT	18. NUMBER OF PAGES	19a. NAME OF RESPONSIBLE PERSON
a. REPORT	b. ABSTRACT	c. THIS PAGE			Leilani Richardson
Unclassified	Unclassified	Unclassified	A		19b. TELEPHONE NUMBER *(include area code)* (661) 275-5015

21 separate items enclosed

9A

MEMORANDUM FOR PRS (In-House/Contractor Publication)

FROM: PROI (TI) (STINFO) 27 September 1999

SUBJECT: Authorization for Release of Technical Information, Control Number: AFRL-PR-ED-TP-FY99-0183, 5895 Mark R. Archambault/Christopher F. Edwards, "Computation of Spray Dynamics by Direct solution of Moment Transport Equations,"

Palace Knight Thesis Research for 38th Annual AIAA ASME Mtg, 10-13 Jan 00

(Statement A)

AIAA-2000-0197

COMPUTATION OF SPRAY DYNAMICS BY DIRECT SOLUTION OF MOMENT TRANSPORT EQUATIONS

Mark R. Archambault*
Propulsion Sciences and Advanced Concepts Division
Air Force Research Laboratory
Edwards AFB, CA 93524

Christopher F. Edwards†
Department of Mechanical Engineering
Stanford University
Stanford, CA 94305

Abstract

In many spray applications, it is important to know the size and velocity distribution of the drops. Conventional particle tracking techniques can require prohibitively large computational times, especially in regions of low droplet number density or when detailed statistics are desired. In this paper, we develop a method to compute the statistics directly by solving a series of moment transport equations. A maximum entropy model is used to close higher-order moments appearing in the equations. Solution of these equations gives not only the transported moments of the spray, but also the maximum entropy probability distribution function from which further statistics can be obtained. The method has been tested on a quasi-one-dimensional spray problem to assess its viability. Submodels which account for the effects of the gas on the drops, including turbulence modification and correlation between the gas and drop velocities, are incorporated. Results for expected quantities are in good agreement with the solution from a particle tracking simulation.

Introduction

Understanding and modeling multiphase flows have become of primary interest in a wide variety of applications. Of particular importance are spray flows such as those associated with liquid fuel injectors, industrial coating processes, and agricultural sprays. A spray flow can be defined as that regime downstream of an injector where a liquid column or sheet has broken up and atomized, but the resultant drops continue to have some mean velocity relative to the gas phase, as opposed to an aerosol where there is no mean slip velocity. Both the liquid phase and the gas phase continue to interact dynamically, exchanging mass, momentum, and energy. This evolution can have a significant impact, for example, on the combustion process inside a liquid rocket engine or on the coating produced by a spray application system. For this reason, it is necessary to have a full understanding of the physics of spray flows and to be able to accurately predict not only the distribution of the drops and their behavior, but also the dynamics of the gas phase, that is, the characteristics of the combined two-phase flow.

Probably the most-used approach in studying spray flows has been the Lagrangian-Eulerian, or particle tracking method.[1,2,3,4] In this approach, the gas phase is predicted by solving the time-dependent, Reynolds-Averaged Navier-Stokes (RANS) equations with a suitable turbulence model and appropriate exchange terms. Drops are stochastically injected into the gas and the drop trajectories are computed by integrating a Lagrangian equation of motion.

While the Lagrangian-Eulerian approach has provided useful information in many applications, it has some significant drawbacks. For instance, data arising from any simulation must be post-processed. If the quantity of interest is the mean number density in each grid cell, this may not pose a problem. However, what if we are interested in the mean number density of drops in a particular size class? The averaging procedure might be simple, but the required computational time is increased because a sufficient number of drops must pass through the cell to provide a data set large enough for a meaningful average. As the quantity of interest becomes more specific, the necessary computation time becomes more prohibitive.

An alternative approach which does not involve simulation is to compute the evolution of a probability density function (PDF) describing the drops. Williams[5]

* Aerospace Engineer
† Assistant Professor

was the first to derive a transport equation for a drop PDF, called the spray equation, analogous to Boltzmann's equation for molecules. However, because obtaining a solution to the spray equation is quite difficult, Williams solved a simplified version of the equation for a steady, one-dimensional spray flow where the gas properties were known in advance. Other solutions[6,7,8,9,10] have been attempted, but with limited success. Because of the high-dimensionality of the spray equation, computations could only be done with a coarse discretization of the phase space.

A different approach to solving the spray equation was taken by Tambour.[11] He only considered the size distribution, but instead of transporting the PDF, he discretized the size axis and derived a set of sectional equations within each size bin. The advantage of this method is that it reduces the dimensionality of the equation to only physical space, though a set of transport equations for each bin has to be solved.

The purpose of this paper is to extend the PDF approach and obtain a complete description of a spray flow by computing the evolution of its PDF along with the gas flow in which it is embedded. This will be accomplished by deriving and solving a set of moment transport equations for average quantities of interest, such as the mean drop velocity and diameter, and developing an appropriate closure model.

Governing Equations

In deriving the equations that will describe the evolution of our system, we will make use of ensemble averaging. This is an averaging procedure that is independent of any time or length scales. We will also restrict ourselves to single-point statistics.[12] Before constructing a probability density function from which average quantities can be obtained, it is necessary to discuss some assumptions about the spray. A single drop can be described by any number characteristics, or marks, such as its size, velocity or temperature. The trade-off, though, is in increasing complexity as more marks are used. Therefore, it is often sufficient to choose a relatively small set of characteristics that contains the information of interest. This set of characteristics prescribes a state vector $\vec{\alpha}$ whose elements define the axes of a hyperspace, called $\vec{\alpha}$-space, through which the drop can move. For example, if the chosen characteristics of the drop are its position in physical space and its diameter, then $\vec{\alpha}=(x_1,x_2,x_3,\phi)$ and $\vec{\alpha}$-space is a four-dimensional hyperspace whose axes are the three position coordinates x_1, x_2, x_3 and the diameter ϕ. As the drop moves through physical space or as it evaporates or condenses, its location in $\vec{\alpha}$-space changes.

Because we are dealing with point particles, volume displacement effects are negligible, and we are able to treat any interphase exchange as if the drop were alone in a locally uniform gas field.

Under these assumptions, a probabilistic description of the spray can be developed,[12] defining $\lambda(\vec{x};t)$[‡] as the probability density of finding a single drop at a point $(\vec{x},t)$. It is also the expected number density of drops at $\vec{x}$ and t. This dual interpretation is important since we are generally more interested in the expected number density rather than the probability density. The probabilistic description also defines a function $f(\vec{\alpha}';\vec{x},t)$, the probability density of finding a particular diameter and velocity, conditioned on a drop existing at $\vec{x}$ and t, where $\vec{\alpha}'$-space is the subset of $\vec{\alpha}$-space excluding the spatial coordinate. By combining these two functions, we define the unnormalized single particle probability density function for the spray

$$F(\vec{\alpha};t)d\vec{\alpha}=\lambda(\vec{x};t)f(\vec{\alpha}';\vec{x},t)d\vec{\alpha}'dV \qquad (1)$$

$F(\vec{\alpha};t)$ is unnormalized because $\lambda(\vec{x};t)$, also an unnormalized PDF, determines how much spray is present at $\vec{x}$ and t.

If $\vec{\alpha}=(\vec{x},\phi,\vec{v},T)$, a transport equation for $F(\vec{\alpha};t)$ can now be derived.[13,14,15]

$$\frac{\partial F}{\partial t}+\nabla_x\cdot(F\vec{v})+\nabla_v\cdot(F\vec{a}) +\frac{\partial}{\partial\phi}(F\Phi)+\frac{\partial}{\partial T}(F\Theta)=\dot{S}_2+\dot{S}_1+\dot{S}_0 \qquad (2)$$

Equation (2) is known as the spray equation. It describes the evolution of the probability distribution function $F(\vec{x},\phi,\vec{v},T;t)$ through joint physical, diameter, velocity, and temperature space and includes source terms accounting for binary collision $\dot{S}_2$, unary breakup $\dot{S}_1$, and zero-body events $\dot{S}_0$ such as nucleation and complete vaporization. The spray equation has not generally been viewed as a practical way of predicting spray flows. It is not an ordinary evolution equation in the sense that the quantity of interest is only being transported through physical space, but also through diameter, velocity, and temperature space. A numerical solution requires a full discretization of this hyperspace. This makes obtaining a direct solution difficult.

Despite the difficulties, attempts have been made at solving the spray equation.[5,6,16,17] Some of these

[‡] For clarity when denoting a PDF, those arguments over which the function is a density will be listed first, followed by a semi-colon, followed by arguments that are parameters of the function.

solutions make use of an assumed form for the PDF F, which leads to a set of transport equations for the parameters that describe the assumed form. The primary problem with this approach is that there is no guarantee that the spray will conform to the assumed distribution throughout its evolution, or even that F can always be described analytically.

However, even the most general PDF can be described by an infinite set of moments. For instance, a one-dimensional distribution's mean determines its location on the axis, its variance is a measure of its width, the third central moment determines the amount of skewness, etc. The value of each moment affects the shape of the distribution in some way, but notice that each higher-order moment affects the shape in a less drastic manner than the next lower-order moment. Thus, it is logical to assume that the lowest-order moments carry sufficient information to reasonably approximate the shape of the distribution as a whole. If it is possible to obtain a function for this shape from these low-order moments, we can then approximate all the other information included in the actual PDF. Then, by solving a set of transport equations for these moments, we can determine how the approximate distribution evolves in time.

Splitting the Spray Equation

Before continuing, we make some simplifying assumptions about the spray. First, we will limit our description of a drop to its spatial location $\vec{x}$, its velocity $\vec{v}$, and its diameter ϕ. Since we are not including the drop temperature, we will only be considering nonvaporizing sprays. The number density of drops will be sufficiently small such that droplet collisions can be neglected. Finally, unary breakup and zero-body source terms will not be considered. These assumptions do not limit the validity of the model–what is left out can be included at any point later on. We make them here for the sake of simplicity.

Upon applying these assumptions to the spray equation (2), we get

$$\frac{\partial F}{\partial t}+\nabla_x\cdot\left(F\vec{v}\right)+\nabla_v\cdot\left(F\vec{a}\right)=0 \tag{3}$$

Substituting equation (1) in the form

$$F\left(\phi,\vec{v},\vec{x};t\right)=\lambda\left(\vec{x};t\right)f\left(\phi,\vec{v};\vec{x},t\right) \tag{4}$$

into (3) and carrying out the product rule gives

$$\begin{aligned}&\lambda\frac{\partial f}{\partial t}+f\frac{\partial\lambda}{\partial t}+\lambda\nabla_x\cdot\left(f\vec{v}\right)+f\vec{v}\cdot\nabla_x\lambda\\&+\lambda\nabla_v\cdot\left(f\vec{a}\right)+f\vec{a}\cdot\nabla_v\lambda=0\end{aligned} \tag{5}$$

By integrating this equation over all velocity and diameter space, i.e. $\vec{\alpha}'$-space, to eliminate f, we obtain

$$\frac{\partial\lambda}{\partial t}+\nabla_x\cdot\left(\lambda\langle\vec{v}\rangle\right)=0 \tag{6}$$

where

$$\langle\vec{v}\rangle=\int_{\vec{\alpha}'}\vec{v}f\left(\vec{\alpha}'\right)d\vec{\alpha}' \tag{7}$$

is the ensemble-averaged, or expected, drop velocity. Equation (6) describes the evolution of the expected number density of drops through space and time. Notice that there is no reference to $\vec{\alpha}'$-space in this equation. The integration has reduced the dimension of the equation from seven (three spatial, one diameter, and three velocity coordinates) to three.

Multiplying equation (6) by f and subtracting the result from equation (5), we get, after rearranging,

$$\begin{aligned}&\frac{\partial f}{\partial t}+\nabla_x\cdot\left(f\vec{v}\right)+\nabla_v\cdot\left(f\vec{a}\right)=\\&f\left[\nabla_x\cdot\langle\vec{v}\rangle+\left(\langle\vec{v}\rangle-\vec{v}\right)\cdot\nabla_x\ln\lambda\right]\end{aligned} \tag{8}$$

This equation describes the evolution of the conditional probability density function through $\vec{\alpha}'$-space. If we interpret (8) as a flow equation, then the first term accounts for the accumulation of probability. The next two terms represent the advection of probability through physical and velocity space, respectively. Additionally, there are two source terms.

The first term on the right side represents the production of probability due to gradients in the mean drop velocity. Suppose that there is a positive gradient in the mean velocity of drops moving through a small volume of physical space. Because of the gradient, drops will be leaving the volume at a greater rate than they enter. This represents a loss of probability. However, f must remain a normalized distribution, by definition. Therefore, probability must be added into the volume without bias towards any droplet characteristic (in proportion to f).

The last term on the right accounts for redistribution of probability in $\vec{\alpha}'$-space due to a gradient in the mean number density of drops. Suppose there is a positive gradient in the mean number density of drops in a volume and the drops have various

velocities. Drops that are moving faster than the mean velocity will leave the volume in greater numbers than those that are moving slower than the mean. Therefore, the probability of finding a fast drop (faster than the mean) decreases while the probability of finding a slow drop (slower than the mean) increases and thus we have a shift of probability in $\vec{\alpha}'$-space.

We now have two equations which, together, are equivalent to equation (3). The equation for the evolution of the mean number density, equation (6), is relatively easy to solve numerically because it has the form of the wave equation for which there are many solution techniques. Conversely, equation (8) presents us with many of the same problems as did (3). In fact, equation (8) appears more complicated than (3). Not only do we still have to solve the equation across all of $\vec{\alpha}$-space, but we have introduced two additional terms. However, as we discuss in the next section, we aren't so much interested in the PDF f itself, but rather various moments of that function. This fact will be used to reduce the dimensionality of equation (8).

Moment Transport Equations

One of the primary motivations behind this study is to compute various statistical averages of interest directly, rather than post-average volumes of simulation data. In this section, we derive a set of moment transport equations. By solving these equations, we are able to calculate the statistical averages at any point in space and time without performing a numerical simulation. Because of space constraints, we only give a cursory derivation here. A detailed derivation can be found in reference [15].

Diameter Moment Transport Equation

Recall that the expected value, or ensemble average, of a quantity $g(k)$ is defined as

$$\langle g \rangle = \int_k g(k) f(k) dk \tag{9}$$

where $f(k)$ is the PDF, and the integral is over the sample space of k. If $g(k)$ is a positive, integer-order power of k, then (9) defines a moment of $f(k)$. In particular, the average drop diameter at some location $\vec{x}$ and t is defined as

$$\langle \phi \rangle = \int_{\phi} \int_{\vec{v}} \phi f(\phi, \vec{v}; \vec{x}, t) d\vec{v} d\phi \tag{10}$$

In the same manner, we can take moments of the transport equation for f. Multiplying equation (8) by ϕ and recognizing that ϕ is an independent coordinate so that it commutes with the derivative operators gives

$$\frac{\partial(\phi f)}{\partial t} + \nabla_x \cdot (\phi f \vec{v}) + \nabla_v \cdot (\phi f \vec{a}) = \phi f \left[\nabla_x \cdot \langle \vec{v} \rangle + (\langle \vec{v} \rangle - \vec{v}) \cdot \nabla_x \ln \lambda \right] \tag{11}$$

Integrating over all diameter and velocity space yields

$$\frac{\partial \langle \phi \rangle}{\partial t} + \nabla_x \cdot \langle \phi \vec{v} \rangle = \langle \phi \rangle \nabla_x \cdot \langle \vec{v} \rangle + \left(\langle \phi \rangle \langle \vec{v} \rangle - \langle \phi \vec{v} \rangle \right) \cdot \nabla_x \ln \lambda \tag{12}$$

This equation describes the evolution of the mean drop diameter through space and time. By making use of equation (6) and the product rule, (12) can be cast in conservative form as

$$\frac{\partial \left(\lambda \langle \phi \rangle \right)}{\partial t} + \nabla_x \cdot \left(\lambda \langle \phi \vec{v} \rangle \right) = 0 \tag{13}$$

Though (13) is an equation for the transport of the mean number density times the mean drop diameter, rather than just the mean drop diameter, it is in a form that is more convenient than equation (12) because it has a form similar to that of the wave equation. Using the same procedure, we can derive transport equations for the second and third moments about the origin for the drop diameter:

$$\frac{\partial \left(\lambda \langle \phi^2 \rangle \right)}{\partial t} + \nabla_x \cdot \left(\lambda \langle \phi^2 \vec{v} \rangle \right) = 0 \tag{14}$$

$$\frac{\partial \left(\lambda \langle \phi^3 \rangle \right)}{\partial t} + \nabla_x \cdot \left(\lambda \langle \phi^3 \vec{v} \rangle \right) = 0 \tag{15}$$

Velocity Moment Transport Equations

Before we can derive equations for the drop velocity moments, we must make some changes to equation (8). It is well understood that droplet velocities correlate with the gas velocities. However, f does not contain any information about the gas. Therefore, we must model the effect the gas phase has on the drops. To do this, we divide the diameter axis into equal-sized "bins" and derive a set of velocity moment equations for each bin. We can then consider the spray as the superposition of a set of monodisperse sprays. This approach is similar to that taken by Tambour[11] when he derived a series of sectional equations, each section representing one bin. Because the drops do not vaporize or breakup, we can justify treating the spray in this manner.

Using conditional probabilities, we split f into two separate probability distributions functions

$$f(\phi,\vec{v};\vec{x},t) = p(\phi;\vec{x},t)q(\vec{v};\phi,\vec{x},t) \tag{16}$$

where $p(\phi;\vec{x},t)d\phi$ is the probability that a drop will be within a diameter interval $d\phi$ centered about ϕ, conditioned on a drop existing at $\vec{x}$ and t, and $q(\vec{v};\phi,\vec{x},t)d\vec{v}$ is the probability that a drop will be within a velocity element $d\vec{v}$ centered about $\vec{v}$, conditioned on a drop with diameter ϕ at $\vec{x}$ and t. Upon substitution of (16) into (8), we have

$$\begin{aligned}&\frac{\partial(pq)}{\partial t}+\nabla_x\cdot(pq\vec{v})+\nabla_v\cdot(pq\vec{a})=\\&pq\left[\nabla_x\cdot\langle\vec{v}\rangle+\left(\langle\vec{v}\rangle-\vec{v}\right)\cdot\nabla_x\ln\lambda\right]\end{aligned} \tag{17}$$

Now let's focus on the n^{th} bin of the diameter axis. Because we have discretized the diameter axis, $p(\phi;\vec{x},t)$ must also be discretized and treated as a constant in each bin, as must be $q(\vec{v};\phi,\vec{x},t)$. We define the binned probability density $f^* = (pq)^*$ as the probability in the bin divided by the width of the bin

$$(pq)^* = \frac{\int_{\phi_n} pq\,d\phi}{\int_{\phi_n} d\phi} = \frac{\int_{\phi_n} pq\,d\phi}{\Delta\phi_n} \tag{18}$$

We also define

$$p^* = \frac{\int_{\phi_n} p\,d\phi}{\int_{\phi_n} d\phi} = \frac{\int_{\phi_n} p\,d\phi}{\Delta\phi_n} \qquad q^* = \frac{(pq)^*}{p^*} \tag{19}$$

We can thus divide equation (17) by $\Delta\phi_n$ and then integrate over the width of the diameter bin to obtain

$$\begin{aligned}&\frac{\partial(p^*q^*)}{\partial t}+\nabla_x\cdot(p^*q^*\vec{v})+\nabla_v\cdot(p^*q^*\vec{a})=\\&p^*q^*\left[\nabla_x\cdot\langle\vec{v}\rangle+\left(\langle\vec{v}\rangle-\vec{v}\right)\cdot\nabla_x\ln\lambda\right]\end{aligned} \tag{20}$$

Multiplying (20) by the drop axial velocity v_x and integrating over all velocity space in the n^{th} diameter bin and defining $\lambda_n = \lambda p^*\Delta\phi_n$ as the mean number density of drops in the n^{th} diameter bin, we arrive at

$$\frac{\partial\left(\lambda_n\langle v_x\rangle_n\right)}{\partial t}+\nabla_x\cdot\left(\lambda_n\langle\vec{v}v_x\rangle_n\right)=\frac{\lambda_n}{\Delta\phi_n}\langle a_x\rangle_n \tag{21}$$

after having made use of equation (6).

The only issue that remains to be addressed is how to handle the momentum exchange terms on the right side of (21). Recall that we have made no assumptions about the spray that limit what we might use for a drag law, allowing us to specify any drag law of interest without significantly changing the equations. For the moment, we will assume that the drops decelerate (or accelerate) according to Stokes' drag law

$$\vec{a} = -\frac{3\pi\mu_g\phi(\vec{v}-\vec{u})}{\frac{\pi}{6}\rho_l\phi^3} = -18\frac{\rho_g\nu_g}{\rho_l\phi^2}(\vec{v}-\vec{u}) \tag{22}$$

where $\vec{u}$ is the gas velocity, μ_g is the gas dynamic viscosity, ρ_g and ρ_l are the gas and liquid densities, respectively, and $\nu_g = \mu_g/\rho_g$ is the gas kinematic viscosity. Using Stokes' drag is not a limitation of the model. Instead, we are using it to keep the analysis simple while we examine the merit of the overall spray model. Substituting equation (22) into (21) gives

$$\begin{aligned}&\frac{\partial\left(\lambda_n\langle v_x\rangle_n\right)}{\partial t}+\nabla_x\cdot\left(\lambda_n\langle\vec{v}v_x\rangle_n\right)\\&=-\frac{\lambda_n}{\tau_n}\left(\langle v_x\rangle_n-\langle u_x\rangle\right)\end{aligned} \tag{23}$$

where

$$\tau_n = \frac{\rho_l\phi_{geo,n}^2}{18\rho_g\nu_g} \tag{24}$$

is the representative droplet relaxation time and $\phi_{geo,n}$ is the geometric mean diameter of the bin.

Similarly, we can write equations for the mean-squared axial velocity, mean transverse velocity, mean-squared transverse velocity, and the axial/transverse velocity cross moment

$$\begin{aligned}&\frac{\partial\left(\lambda_n\langle v_x^2\rangle_n\right)}{\partial t}+\nabla_x\cdot\left(\lambda_n\langle\vec{v}v_x^2\rangle_n\right)\\&=-2\frac{\lambda_n}{\tau_n}\left(\langle v_x^2\rangle_n-\langle u_xv_x\rangle_n\right)\end{aligned} \tag{25}$$

$$\begin{aligned}&\frac{\partial\left(\lambda_n\langle v_y\rangle_n\right)}{\partial t}+\nabla_x\cdot\left(\lambda_n\langle\vec{v}v_y\rangle_n\right)\\&=-\frac{\lambda_n}{\tau_n}\left(\langle v_y\rangle_n-\langle u_y\rangle\right)\end{aligned} \tag{26}$$

$$\frac{\partial\left(\lambda_n\left\langle \mathrm{v}_y^2\right\rangle_n\right)}{\partial t}+\nabla_x\cdot\left(\lambda_n\left\langle \bar{\mathrm{v}}\mathrm{v}_y^2\right\rangle_n\right) = -2\frac{\lambda_n}{\tau_n}\left(\left\langle \mathrm{v}_y^2\right\rangle_n-\left\langle u_y\mathrm{v}_y\right\rangle_n\right) \tag{27}$$

$$\frac{\partial\left(\lambda_n\left\langle \mathrm{v}_x\mathrm{v}_y\right\rangle_n\right)}{\partial t}+\nabla_x\cdot\left(\lambda_n\left\langle \bar{\mathrm{v}}\mathrm{v}_x\mathrm{v}_y\right\rangle_n\right) = -\frac{\lambda_n}{\tau_n}\left(2\left\langle \mathrm{v}_x\mathrm{v}_y\right\rangle_n-\left\langle \mathrm{v}_x u_x\right\rangle_n-\left\langle \mathrm{v}_y u_y\right\rangle_n\right) \tag{28}$$

Equations (6), (13) through (15), (23), and (25) through (28) are the set of equations that we will use to describe the evolution of the spray droplet PDF. However, because we can treat each bin as a separate spray, equation (6) holds in each bin, using each bin's mean drop velocity $\langle\bar{\mathrm{v}}\rangle_n$ and number density λ_n. Because the overall number density is the sum of the binned number densities and $\lambda_n=\lambda p^*\Delta\phi_n$, we can reconstruct the diameter PDF from the binned number densities. This alleviates our need to solve the diameter moment transport equations (13), (14), and (15).

Maximum Entropy Moment Closure (MEMC)

This moment method is based on a hierarchical moment structure similar to that encountered in turbulence modeling. As each successive moment transport equation is derived, at least one new, higher-order moment is introduced. These unclosed moments can be evaluated by making use of the Maximum Entropy Formalism (MEF). In his study of communications theory, Shannon[18] developed the concept of information entropy as a measure of probabilistic uncertainty. For a continuous distribution, this measure is given by

$$S=-\int_a^b f(x)\ln f(x)dx \tag{29}$$

Later, Jaynes[19] showed that an infinite number of PDFs are consistent with a set of known constraints, but that the one that should be chosen is the one with maximum entropy. If a PDF with less entropy (i.e., less uncertainty) were used, it would imply the existence of some additional knowledge. However, since all the available knowledge was applied in the form of constraints, no additional knowledge would exist. Thus it would be inappropriate to choose any PDF other than the one with maximum entropy. This PDF is the most unbiased distribution possible within the given constraints.

Because they have the greatest influence on the shape of the PDF, we will constrain the lowest-order moments (i.e. means, variances, etc.). These moments correspond to those for which we have derived transport equations. Equation (29) is maximized by way of the method of Lagrange multipliers. This leads to a PDF of the form

$$f=\exp\left[-\beta_0-\sum_{r=1}^{M}\beta_r g_r(\bar{\alpha}')\right] \tag{30}$$

where the β's are the Lagrange multipliers, $g_r(\bar{\alpha}')$ is the r^{th} functional quantity to be averaged, and M is the number of moment constraints. The coefficients are determined from a non-linear system of coupled differential equations which, in general, must be solved numerically.

Sellens[20] and Chin et. al.[21] have made use of the MEF in their work on predicting droplet distributions resulting from breakup of a liquid sheet or jet. In this work, the breakup process is considered independently from gas-phase constraints, and it is not their intention to solve for the evolution of the droplet distribution throughout space and time, but rather to obtain a distribution for all the drops in the spray. In contrast, our work is focused on describing the *evolution* of a droplet PDF at every point in the flow domain and how that evolution is influenced by and interacts with the gas phase. In our approach, we model the evolution of the complete, coupled spray flow using moment equations. The MEF is introduced as a method to close those equations.

Quasi-One-Dimensional Spray Problem

To explore the usefulness of this approach, we make use of a quasi-one-dimensional spray flow. The purpose of this is to pose a spray problem that is understandable, physically interesting, and tractable. Moreover, we wish to look at a simple problem to determine if there are any flaws in the proposed closure models which will present themselves more readily in this problem than in a more complicated, multi-dimensional problem.

Figure (1) shows the geometry for this problem. At $x=0$ there is a two-dimensional array of spray injectors that extends infinitely in the y-direction. Each injector has been placed at random on this array and points in the x-direction, delivering a distribution of drops into an incompressible gas, which initially has a low level of turbulence. The array and each injector on it extend infinitely in z-direction, resulting in a series of wedge sprays of spherical drops.

Now imagine an ensemble of these arrays where, on each, the injectors have been placed at random. Because we wish to develop a quasi-one-dimensional

flow, we restrict the PDF for the drop velocities at each injector to have a mean transverse (y-direction) velocity of zero. If there is an infinite number of realizations in the ensemble, then there is no preferential location along the transverse axis since there is equal probability for a drop to have a positive y-velocity of some magnitude as there is for a drop to have a negative y-velocity of the same magnitude. Similarly, we have a zero-mean gas velocity component in the y-direction, though fluctuations do occur. Because there is no preferential location along the transverse axis, there are no variations along that axis *across the ensemble*, and therefore, derivatives of averaged quantities in the y-direction are zero. So, the three primary constraints we have for this problem are

$$\langle u_y \rangle = 0, \quad \langle \mathrm{v}_y \rangle = 0, \quad \frac{\partial \langle\ \rangle}{\partial y} = 0 \tag{31}$$

Also, so that no mean flow develops in the transverse direction, there can be no correlation between the x- and y-components of velocity in either phase. Thus, all cross-component and cross-component/cross-phase moments (i.e. $\langle \mathrm{v}_x \mathrm{v}_y \rangle, \langle u_x \mathrm{v}_y \rangle$, etc.) equal zero. Substituting these constraints into the velocity moment transport equations yields

$$\frac{\partial \lambda_n}{\partial t} + \frac{\partial \left(\lambda_n \langle \mathrm{v}_x \rangle_n \right)}{\partial x} = 0 \tag{32}$$

$$\frac{\partial \left(\lambda_n \langle \mathrm{v}_x \rangle_n \right)}{\partial t} + \frac{\partial \left(\lambda_n \langle \mathrm{v}_x^2 \rangle_n \right)}{\partial x} = -\frac{\lambda_n}{\tau_n} \left(\langle \mathrm{v}_x \rangle_n - \langle u_x \rangle \right) \tag{33}$$

$$\begin{aligned} &\frac{\partial \left(\lambda_n \langle \mathrm{v}_x^2 \rangle_n \right)}{\partial t} + \frac{\partial \left(\lambda_n \langle \mathrm{v}_x^3 \rangle_n \right)}{\partial x} \\ &= -2 \frac{\lambda_n}{\tau_n} \left(\langle \mathrm{v}_x^2 \rangle_n - \langle u_x \mathrm{v}_x \rangle_n \right) \end{aligned} \tag{34}$$

$$\begin{aligned} &\frac{\partial \left(\lambda_n \langle \mathrm{v}_y^2 \rangle_n \right)}{\partial t} + \frac{\partial \left(\lambda_n \langle \mathrm{v}_x \mathrm{v}_y^2 \rangle_n \right)}{\partial x} \\ &= -2 \frac{\lambda_n}{\tau_n} \left(\langle \mathrm{v}_y^2 \rangle_n - \langle u_y \mathrm{v}_y \rangle_n \right) \end{aligned} \tag{35}$$

If constraints (31) are applied to the incompressible RANS equations, we obtain

$$\frac{\partial \langle u_x \rangle}{\partial x} = 0 \tag{36}$$

$$\frac{\partial \langle u_x \rangle}{\partial t} = -\frac{\partial \langle P \rangle}{\partial x} - \frac{\partial \langle u_x'^2 \rangle}{\partial x} + 3\pi v_g \lambda \left\langle \phi \left(\mathrm{v}_x - u_x \right) \right\rangle \tag{37}$$

Equation (36) says that the mean gas velocity is a constant in space. If we specify the inlet mean gas velocity as a constant in time, then the mean gas velocity throughout the domain is constant in both space and time. This makes solving the gas momentum equation unnecessary unless one is interested in the pressure. Since our present interests are in the discrete phase and not the gas, we do not need to solve equations (36) and (37). However, a $k-\varepsilon$ turbulence model, modified to account for the drops,[3] is solved since the gas-phase turbulence is incorporated into the cross-phase moments appearing in equations (34) and (35).

The moment equations are solved using an implicit, first-order, upwind scheme for the spatial derivatives and a second-order backwards difference for the time derivatives. A first-order scheme was chosen for the spatial derivatives due to the difficulties associated with solving moment equations. Moment variables have relations among them that must be preserved, constraining their values. For example, the relation between the first and second moment of a PDF is

$$\langle X^2 \rangle - \langle X \rangle^2 \geq 0 \tag{38}$$

where X is any random variable. If this relation is not maintained, then the numerical solution may either become unstable or give non-physical answers. Second-order numerical solutions of hyperbolic equations can cause oscillations in the solution in regions of strong gradients, even when artificial dissipation is added. Being non-physical, those oscillations could cause the numerical solution of the variance to become negative, corrupting the remainder of the solution.

For comparison, a Lagrangian simulation of the quasi-one-dimensional spray is performed. Individual drops are tracked from the injector along their trajectories. Because the mean gas velocity is a constant in space and time, the gas momentum and continuity equations are not solved, though a $k-\varepsilon$ model is used to simulate the turbulence, giving each drop a random "kick" over a duration equal to the eddy turnover time or the drop residence time, whichever is shorter.

Results

Table 1 lists the moments used to specify the droplet PDF at the injector and the gas phase characteristics. The diameter PDF is shown in Figure 2

and the velocity PDFs are Gaussian. The inlet condition for the turbulent kinetic energy corresponds to a RMS value of five percent of the mean gas velocity and the rate of dissipation of turbulent kinetic energy is $\varepsilon = k/100\,\mathrm{sec}$.

Figure 3 shows profiles of the mean number density. It is clear where the leading edge of the spray is at each time interval and how it propagates through the domain as a concentration wave. The mean number densities behind it are much greater than the injection mean number density. This is what we would expect since the drops are injected into a slower gas. The drops rapidly decelerate and accumulate just behind the leading edge. This accumulation of drops continues until the drops have been slowed to the mean gas velocity. The results compare well with the Lagrangian simulation in the region behind the leading edge. At the leading edge, the MEMC results deviate from the simulation. However, this is due to the numerical dissipation associated with the first-order numerical scheme.

At the leading edge, the mean number density is quite low. When drops first arrive at some spatial location, only a few are present, those that were large enough not to have been greatly influenced by drag. This is shown in Figure 4 where the expected drop diameter is plotted. At the leading edge, there is a greater mean drop diameter. This is caused by the strong slip velocity present in the flow, decelerating all but the most massive drops. As we move upstream, we encounter the smaller drops that were quickly decelerated.

Figure 5 shows how the standard deviation of the diameter PDF evolves. At the leading edge, the standard deviation is large. This comes from the fact that there are so few drops out on the wave front. Those drops present are large due to the developed size-velocity correlation. Figure 2 shows that there is a wide range of large diameters that those drops have. It can be argued that the shape of the standard deviation curve behind the leading edge is a phenomenon that arises from the spatial spreading of the drops that were initially injected, however, because the numerical diffusion at the leading edge, this effect may appear more significant than it really is.

Figure 6 shows the mean drop axial velocity profiles. The region closest to the injector is where the highest velocity slip occurs. There are a number of drops passing through this region that are moving faster than the mean gas velocity. Due to their lower masses, most of those drops rapidly decelerate, reducing the mean velocity. The mean velocity of these drops approaches the mean gas velocity within 3 meters. At the leading edge, however, the mean velocity again begins to increase. To have reached the leading edge, those drops had to be the fastest coming out of the injector, and because they are also some of the largest, they haven't been affected by drag as much as the smaller drops. Thus, the mean velocity is higher at the edge. As the wave front continues to move forward, those large drops slow as evidenced by the decrease in the mean velocity on the front as time goes on.

Figures 7 and 8 show the standard deviations of the axial and transverse velocity distribution functions. They are measures of the width of the velocity PDFs. The larger widths occur near the injector because the drops have not been influenced by the gas phase long enough to have approached the gas velocity. Downstream, the standard deviations rapidly decay until we reach the wave front. It will take a longer time for the larger drops to reach the gas velocity, but as the leading edge propagates, the standard deviations become smaller and smaller. Again, there is good agreement with the simulation.

One thing of note is the magnitude of the drop axial velocity standard deviation relative to the mean drop velocity. At the injector, the standard deviation was prescribed as one-tenth of the injection mean. In Figure 7, however, we see it is much wider in the region of strong slip. This results from the fast drops quickly moving ahead, and slower ones lagging. Many drops close to the injector have decelerated, especially the smallest ones. There is also a significant number of larger drops in this region that are moving with velocities closer to the mean injection velocity or faster. Most of these drops are the more massive ones not having been greatly influenced by drag as yet. Thus, in the region of strong slip, there is a much wider distribution of velocities as a result of deceleration. This is the reason for the much higher axial velocity standard deviation.

The simulation results in the figures are the averages of ten runs. Because of the nature of the simulation, and because the results are averages of only a few realizations, there is a great deal of noise in the simulation data. To smooth this out, and to better approximate an ensemble average, we would ideally like to average over thousands of simulations. However, because of the computational time required, we are prohibited from doing this. The best we can do is time average, but we are limited to doing this only in regions that have reached a steady state. We are not able to capture the averaged dynamics of the leading edge using a simulation unless we ensemble average. This is a significant advantage that the current model has over the Lagrangian simulation.

A second advantage is the savings in computational time for getting detailed statistics. Because we always

have an approximation to the PDF as part of the solution to the MEMC model, we can, at any time, integrate that PDF and obtain any statistics of interest. This is not true with the Lagrangian simulation, since, as the level of statistical detail increases, so does the time required to collect sufficient data. Figure 9 compares the nondimensional times required to obtain different types of statistics between the two models for this problem. Other problems may have different timt results, though the general trends will be the same. The MEMC calculation was run for six seconds of flow time. Bar A represents the time required to run the simulation for the same amount of flow time and obtain a "snapshot" of the simulation at that point. Bar B denotes the amount of time required to get steady-state statistics at all grid locations up to 100 mm. Bars C and D show the time needed to obtain more detailed steady-state statistics up to 100 mm downstream of the injector. In case C, statistics were computed only on drops with a diameter greater than 100 μm and in case D, only on drops with a diameter greater than 100 μm and a velocity greater than 23 mm/s. Note that as the level of detail increases, so does the simulation time. To obtain averaged data from the simulation for the transient region requires an even greater amount of time since we must ensemble average this region, requiring many simulation runs.

Conclusions

We have developed a model which describes the evolution of a spray flow by transporting a series of moments of the droplet probability density function and closing those equations with a maximum entropy model. The model was tested on a quasi-one-dimensional spray and results for several quantities of the spray were obtained, including the expected number density, expected droplet diameter, and expected droplet velocity. We obtained acceptable agreement with statistical data obtained from a Lagrangian simulation, both in the steady-state regions and the transient region. We also showed that the present model can offer a significant computational time saving over a simulation when detailed statistics are desired.

References

1. Dukowicz, J. K., "A Particle-Fluid Numerical Model for Liquid Sprays," *J. Comp. Phys.*, vol. 35, pp 229-253, 1980.

2. Gosman, A. D., & Ioannides, E., "Aspects of Computer Simulation of Liquid Fueled Combustors," *J. Energy,* vol. 7, pp. 482-490, 1983.

3. Amsden, A. A., O'Rourke, P. J., & Butler, T. D., "KIVA-II: A Computer Program for Chemically Reactive Flows with Sprays," Los Alamos National Laboratory, Report No. LA-11560-MS, Los Alamos, NM, 1989.

4. Berlemont, A., Desjonqueres, P., & Gouesbet, G., "Particle Lagrangian Simulation in Turbulent Flows," *J. Multiplahse Flow*, vol. 16, pp. 19-34, 1990.

5. Williams, F. A., "Spray Combustion and Atomization," *Phys. Fluids*, vol. 1, pp. 541-545, 1958.

6. Bracco, F. V., Gupta, H. C., Krishnamurthy, L., Santavicca, D. A., Steinberger, R. L., & Warshaw, V. "Two-Phase, Two-Dimensional, Unsteady Combustion in Internal Combustion Engines; Preliminary Theoretical-Experimental Results," SAE paper 760114, 1976.

7. Westbrook, C. K., "Three Dimensional Numerical Modeling of Liquid Fuel Sprays," *Sixteenth Internat. Symp. Combust.*, Cambridge, 1976.

8. Gupta, H. C., & Bracco, F. V., "Numerical Computations of Two-Dimensional Unsteady Sprays for Application to Engines," *AIAA J.*, vol. 16, pp. 1053-1061, 1978.

9. Haselman, L. C., & Westbrook, C. K., "A Theoretical Model for Two-Phase Fuel Injection in Stratified Charge Engines," SAE paper 780318, 1978.

10. Sirignano, W. A., "The Formulation of Spray Combustion Models: Resolution Compared to Droplet Spacing," *J. Heat Transfer*, vol. 108, pp. 633-639, 1986.

11. Tambour, Y., "A Sectional Model for Evaporation and Combustion of Sprays of Liquid Fuels," *Isr. J. Technol.*, vol. 18, pp. 47-56, 1980.

12. Edwards, C. F., & Marx, K. D., "Single-Point Statistics of Ideal Sprays, Part I: Fundamental Descriptions and Derived Quantities," *Atomization and Sprays*, vol. 6, pp. 499-536, 1996.

13. Williams, F. A., *Combustion Theory*, 2nd ed., The Benjamin/Cummings Publishing Company, Menlo Park, CA, 1985.

14. O'Rourke, P. J., "Collective Drop Effects on Vaporizing Liquids Sprays," Ph.D. thesis, Princeton University, Princeton, NJ, 1981.

15. Archambault, M. R., "A Maximum Entropy Moment Closure Approach to Modeling the Evolution of Spray Flows," Ph.D. thesis, Stanford University, Stanford, CA 1999.

16. Travis, J. R., Harlow, F. H., Amsden, A. A., "Numerical Calculation of Two-Phase Flows," *Nuclear Sci. Eng.*, vol. 61, pp. 1-10, 1976.

17. Groeneweg, J. F., "The Statistical Description of a Spray in Terms of Drop Velocity, Size, and Position," Ph.D. thesis, Univ. of Wisconsin, 1967.

18. Shannon, C. E., "A Mathematical Theory of Communications," *Bell Syst. Tech. J.*, vol. 27, pp 379-623, 1948.

19. Jaynes, E. T., "Information Theory and Statistical Mechanics," *Phys. Review*, vol. 106, pp. 620-630, 1957.

20. Sellens, R. W., "Prediction of the Drop Size and Velocity Distribution in a Spray, Based on the Maximum Entropy Formalism," *Part. Part. Syst. Charact.*, vol. 6, pp. 17-27, 1989.

21. Chin, L. P., Hsing, P. C., Tankin, R. S., & Jackson, T., "Comparisons Between Experiments and Predictions Based on Maximum Entropy for the Breakup of a Cylindrical Liquid Jet," *Atomization and Sprays*, vol. 5, pp. 603-620, 1995.

λ	$1000\ \frac{drops}{cm^3}$	σ_{v_x}	$0.015 m/s$
$\langle\phi\rangle$	$100\,\mu m$	σ_{v_y}	$0.015 m/s$
$\langle\phi^2\rangle$	$150\,\mu m$	$\langle u_x\rangle$	$0.0225 m/s$
$\langle\phi^3\rangle$	$300\,\mu m$	$\langle u_y\rangle$	$0.0 m/s$
$\langle v_x\rangle$	$0.15 m/s$	σ_{u_x}	$1.15 mm/s$
$\langle v_y\rangle$	$0.0 m/s$	σ_{u_y}	$1.15 mm/s$

Table 1 Injector Conditions

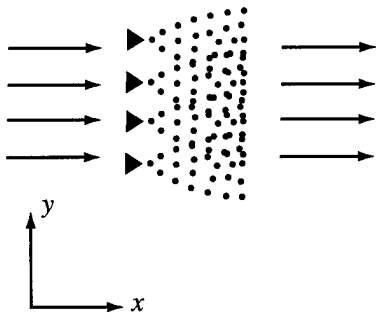

Figure 1 Geometry for quasi-1D spray flow

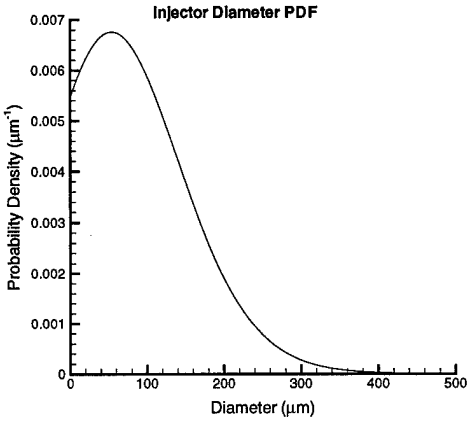

Figure 2 Injector diameter PDF

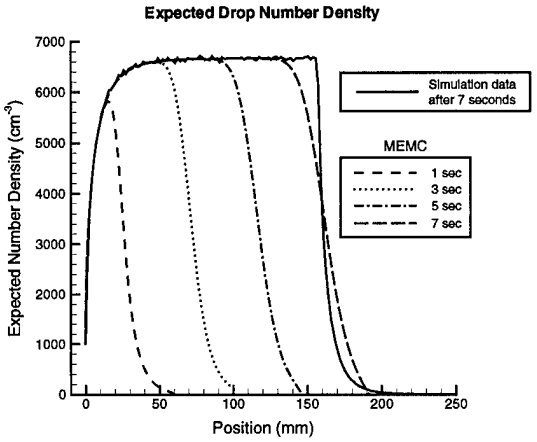

Figure 3 Mean drop number density

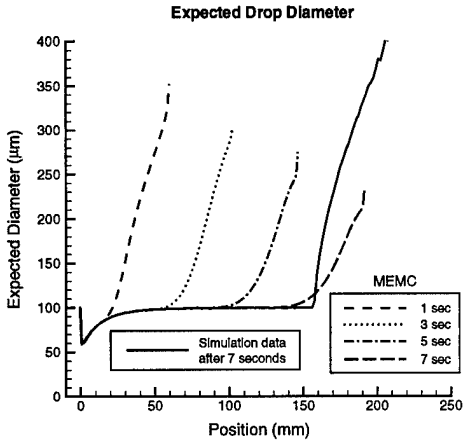

Figure 4 Mean drop diameter

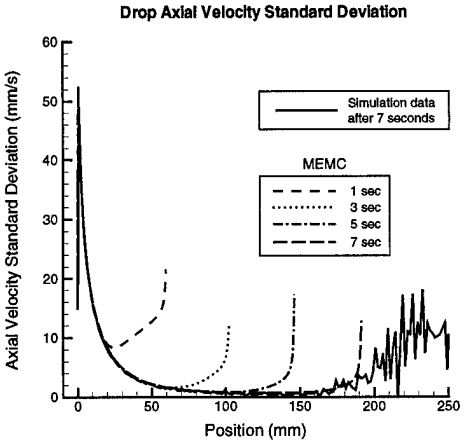

Figure 7 Drop axial velocity standard deviation

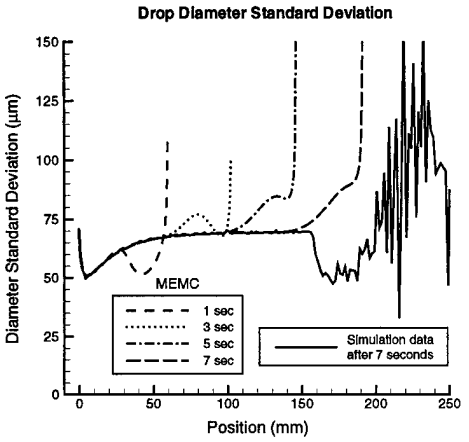

Figure 5 Drop diameter standard deviation

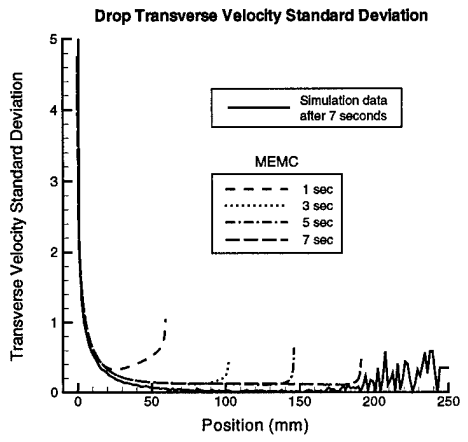

Figure 8 Drop transverse velocity standard deviation

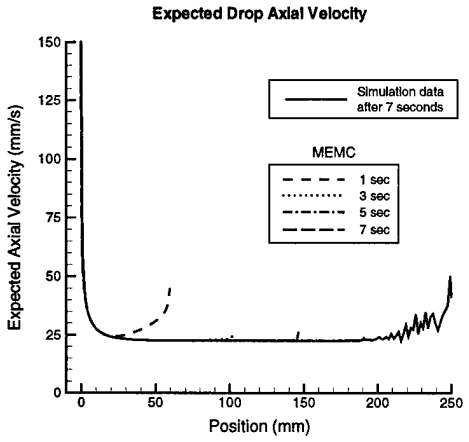

Figure 6 Mean drop axial velocity

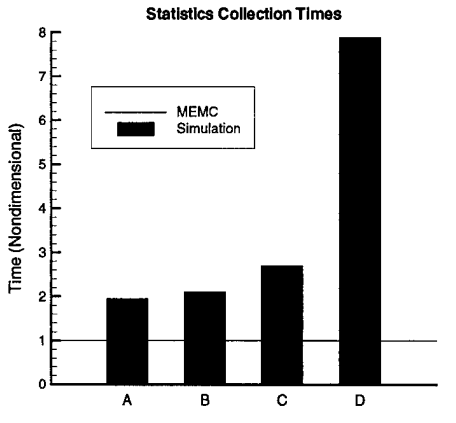

Figure 9 Simulation vs. MEMC computational times.